Research Article

Muhammad Hanif Sainorudin, Nur Athirah Abdullah, Mohd Saiful Asmal Rani, Masita Mohammad*, Munirah Mahizan, Nursyazwani Shadan, Nurul Huda Abd Kadir*, Zahira Yaakob, Adel El-Denglawey*, and Mahboob Alam*

Structural characterization of microcrystalline and nanocrystalline cellulose from *Ananas comosus* L. leaves: Cytocompatibility and molecular docking studies

https://doi.org/10.1515/ntrev-2021-0053
received May 27, 2021; accepted July 15, 2021

Abstract: The present study focused on the preparation of microcrystalline cellulose (MCC) and nanocrystalline cellulose (NCC) from pineapple (*Ananas comosus* L.) leaves using chemical treatments followed by acid hydrolysis. Pineapple leaves could be used in medical applications such as drug delivery carriers. Advanced spectroscopy techniques such as Fourier-transform infrared (FT-IR), X-ray diffraction (XRD), scanning electron microscopy (SEM), and transmission electron microscopy (TEM) were used to analyze the physical, chemical, and morphological features of the isolated MCC and NCC; the results indicated the needle-shaped form of nanostructures with good purity and high crystallinity index of 75.00 and 76.38%, respectively. In addition, inhibition of the treated MRC-5 cells with all the samples revealed that the percentage of cell viability was less than 30%, which is an interesting finding given their role in the cytotoxicity effect of MCC and NCC. It appears that MCC and NCC derived from pineapple leaves have lower toxicity. As a result, the developed MCC and NCC can be used in pharmaceutical applications as a novel drug delivery system. Molecular docking was performed to understand the non-bonding interaction of cellulose with human acid-beta-glucosidase (β-Glc) (PDB: 1OGS). The docking result shows that cellulose unit docked within the active pocket of the enzyme by forming hydrogen bonds against ASN19, THR21, and VAL17 with distances of 2.18, 1.93, and 2.92 Å, respectively, with binding energy (−5.0 kcal/mol) resulting in close interaction of cellulose unit with the receptor.

Keywords: cytotoxicity, MCC, NCC, pineapple leaves, molecular docking

*** Corresponding author: Masita Mohammad,** Solar Energy Research Institute, Universiti Kebangsaan Malaysia, 43600, Bangi, Selangor, Malaysia, e-mail: masita@ukm.edu.my
*** Corresponding author: Nurul Huda Abd Kadir,** Faculty Science and Marine Environment, Universiti Malaysia Terengganu, 21030 Kuala Nerus, Terengganu, Malaysia, e-mail: nurulhuda@umt.edu.my
*** Corresponding author: Adel El-Denglawey,** Department of Physics, College of University College at Turabah, Taif University, P.O. Box 11099, Taif 21944, Saudi Arabia, e-mail: a.denglawey@tu.edu.sa, denglawey@yahoo.com
*** Corresponding author: Mahboob Alam,** Division of Chemistry and Biotechnology, Dongguk University, 123 Dongdae-ro, Gyeongju-780-714, Republic of Korea, e-mail: mahboobchem@gmail.com
Muhammad Hanif Sainorudin, Nur Athirah Abdullah: Solar Energy Research Institute, Universiti Kebangsaan Malaysia, 43600, Bangi, Selangor, Malaysia
Mohd Saiful Asmal Rani: Solar Energy Research Institute, Universiti Kebangsaan Malaysia, 43600, Bangi, Selangor, Malaysia; School of Materials and Mineral Resources Engineering, Engineering Campus, Universiti Sains Malaysia, 14300 Nibong Tebal, Penang, Malaysia
Munirah Mahizan: Institute of Systems Biology, Universiti Kebangsaan Malaysia, 43600, Bangi, Selangor, Malaysia
Nursyazwani Shadan: Faculty Science and Marine Environment, Universiti Malaysia Terengganu, 21030 Kuala Nerus, Terengganu, Malaysia
Zahira Yaakob: Department of Chemical and Process Engineering, Faculty of Engineering and Built Environment, Universiti Kebangsaan Malaysia, 43600, Bangi, Selangor, Malaysia

1 Introduction

The growing interest in cellulose-based products from a sustainable, renewable, and environmentally friendly source has placed cellulose on top of attractive nanomaterials for commercialization in recent years. Extensive use of nanomaterials produced from natural fibres has improved its properties and generated new commercial products. A new approach, however, is possible of the

use of biodegradable and easily recyclable materials for the convenience of human life. Many of the building blocks widely used in understanding communication and electronic hardware are made from these cellulose-based materials. Still, it has also shown increasing importance in human exposure, specifically as a drug delivery carrier [1,2]. Cellulose that can be isolated from agricultural wastes needs excellent attention and it has the potential to open up new opportunities for advanced technologies in the biomedical industry [3]. It is a natural biopolymer that is most abundant on the Earth, relatively inexpensive, and widely used as a medicinal excipient aiding the release of prolonged and regulated drugs [4]. Despite the fact that earlier research has concluded that cellulose has minimal or low toxicity in the use as biomedical materials [5,6], concerns regarding cytotoxicity and biosafety should be further focused on these natural nanomaterials.

Several strategies for extracting cellulose from lignocellulosic biomass and modifying cellulosic derivatives in order to produce micro and nanocrystalline cellulose (MCC and NCC) with higher purity and crystallinity degrees have been reported [7]. On the other hand, their versatility and ability to modify physicochemical qualities increased the potential of MCC and NCC to be used in various applications. The utilization of cellulose for drug delivery is an active area of research since they own notable physical features, unique chemical surface characteristics, and even excellent biological properties [8]. Generally, cellulose is composed of β-1,4 glycosidic unit bonds. Cellulose can be purified and isolated from plant cell walls and have unique physicochemical and structural characteristics that make it possible to be used in advanced nanomaterials [9] and nanoengineering applications [3]. Linear chains of cellulose microfibrils combine to form a region consisting of disordered (amorphous) and highly ordered (crystalline) structures. Once the crystals of cellulose are removed from biomass such as pineapple leaves, terminologies such as MCC and NCC can be recognized based on the size of its molecules [10]. Exclusion of the amorphous region influences the structure and crystallinity of the cellulose fibres [11]. Natural cellulose derived from biomass can be processed into micro- and nanosized materials like MCC and NCC possessing good properties for specific applications [12,13] and expected to have low or non-toxicity.

With the increasing presence of MCC and NCC in consumer products, it is important to determine and confirm the safety of these materials to be used in pharmaceutical applications. Cellulose-based materials like MCC and NCC must be non-toxic to the human body. The finding regarding *in vitro* studies for MCC and NCC derived from pineapple leaves on normal cells is still lacking. The potential used as the drug carrier system is limited, as well as the development of MCC and NCC from pineapple leaves for drug delivery carriers is not fully explored. Since the pineapple plant (*Ananas comosus*) is among the nutrient-richest plant, they offer many benefits in biomedical applications [14]. In Malaysia, the pineapple plant is harvested annually for its fruit, and the remaining parts are disposed of as agricultural waste, such as leaves. The pineapple leaf fibre obtained from the leaves of the pineapple plant, which comes from the Bromeliaceae family [15], is very hygroscopic, widely available, and of low cost, and can be considered a natural fibre that exhibits high specific strength and rigidity.

Pineapple plants are overwhelmingly valuable species and are the most prominent tropical fruits in the world. The use of its waste as the primary source of substitute fibre production is very promising. Pineapple plantations produce many leaves during the post-harvesting that can be used for high fibre-based materials. This waste, if not used properly, will bring a negative impact on the environment. Cellulose isolated from this type of agro-wastes permits the formation of high-purity crystals[16]. The physical appearance of pineapple leaves is waxy, 50–180 cm long, sword-like, and have sharp thorns on the edges that are arranged in a rosette around the stem, and the colour varies from a uniform green to red, yellow, or ivory of the striped as shown in Figure 1. Pineapple (*Ananas comosus* L.) leaves are among a plant residue containing high cellulose, almost identical with coconut husk and sugarcane bagasse [17].

Alternatives cheap and readily available raw materials are needed to replace the limited source of petroleum-based products. Countries grow crops and fruits not only for agricultural purposes but also to produce raw materials for industries [18]. Many developing countries trade in cellulose fibres to improve the economic condition

Figure 1: Photograph of *Ananas comosus* plant.

of poor farmers with support from the country [19]. This work aims to investigate the safety and cytotoxicity assessment of MCC and NCC derived from pineapple leaves for biomedical purposes, as the isolation of cellulose from pineapple leaves for medical use has not been widely explored. Moreover, this work can provide important information in planning further studies on MCC and NCC to see its suitability and compatibility in the application of the drug delivery system. Furthermore, molecular docking of cellulose units was carried out in order to interact with human acid-beta-glucosidase (PDB: 1OGS). The study of these interactions will be beneficial and will provide ideas for biomedical purposes, especially in order to understand human cells compatibility in tissue generation as well as for drug delivery. The MCC and NCC derived from various raw materials using different acid hydrolysis methods, including crystallinities are presented in Table 1 as documented elsewhere.

2 Materials and methods

2.1 Materials

The pineapple leaf wastes were collected and supplied by the local village area, Dengkil (Selangor, Malaysia). RPMI 1640, penicillin/streptomycin, and foetal bovine serum (FBS) were purchased from Naqalai Tech, Japan; and phosphate-buffered saline (PBS) and 0.25% trypsin-EDTA were purchased from Sigma Aldrich, (UK). The MTT reagent was purchased from Merck (Germany). Hydrochloric acid (HCl), sulphuric acid (H_2SO_4), sodium hydroxide (NaOH), sodium hypochlorite (NaClO), hydrogen peroxide (H_2O_2), and dimethyl sulphoxide (C_2H_6OS) were bought from Sigma Aldrich, UK. Unless otherwise stated in the text, all other chemicals were purchased from R&M Chemicals, Germany.

2.2 Isolation of MCC and NCC

Figures 2 and 3 illustrate several procedures leading to the preparation of MCC and NCC from pineapple leaves. The raw samples of pineapple leaves were obtained and washed in distilled water for purification. The samples were then dried in an oven for over 48 h at a temperature of 60°C. Then, the dried samples were ground in a grinder machine and sieved until the required powder sizes were reached. The samples were packed in a plastic polyethylene bag and then placed at room temperature for further processing [36]. The steps outlined below and in Figure 2 were used to prepare and purify MCC from pineapple leaves. Step (1) 15 g of samples were added with 2 wt% of NaOH for 5 h at 80°C. Step (2) The material was washed three times with distilled water, filtered with Whatman paper, and dried in a hot air oven at 60–65°C until it

Table 1: Essential sources of lignocellulosic biomass for crystalline cellulose production

Raw materials	Methods	Types of crystalline cellulose formed with *CI%	*Ref.
Eucalyptus pulp	Sulphuric acid	MCC and NCC	[20]
Pomelo peel	Hydrochloric acid	MCC with 40.5	[21]
Roselle fibres	Hydrochloric acid	MCC with 78	[22]
Corn cob	Hydrochloric acid Sulphuric acid	MCC	[23]
Cotton gin waste	Hydrochloric acid Sulphuric acid	MCC	[24]
Alfa fibres	Hydrochloric acid	MCC with 73.6	[25]
Oil palm biomass	Sulphuric acid	MCC with 87	[26]
Bacterial cellulose from acetobacter xylinum	Sulphuric acid	MCC with 69	[27]
Pineapple crown leaf	Sulphuric acid	NCC with 78.21	[28]
Pineapple peel residues	Hydrochloric sulphuric acid	NCC	[29]
Tomato stem	Sulphuric acid	NCC with 74.4	[30]
Wheat stalk	Sulphuric acid	MCC and NCC	[31]
Rice husk	Sulphuric acid	NCC with 65	[31]
Sugarcane bagasse	Sulphuric acid	NCC with 68.28	[32]
Sugar palm fibres	Sulphuric acid	NCC with 85.9	[33]
Rose stem	Alkaline peroxide	MCC with 65.4	[34]
Date seeds	Hydrochloric	MCC with 70	[35]

*CI: crystallinity index, Ref.: references.

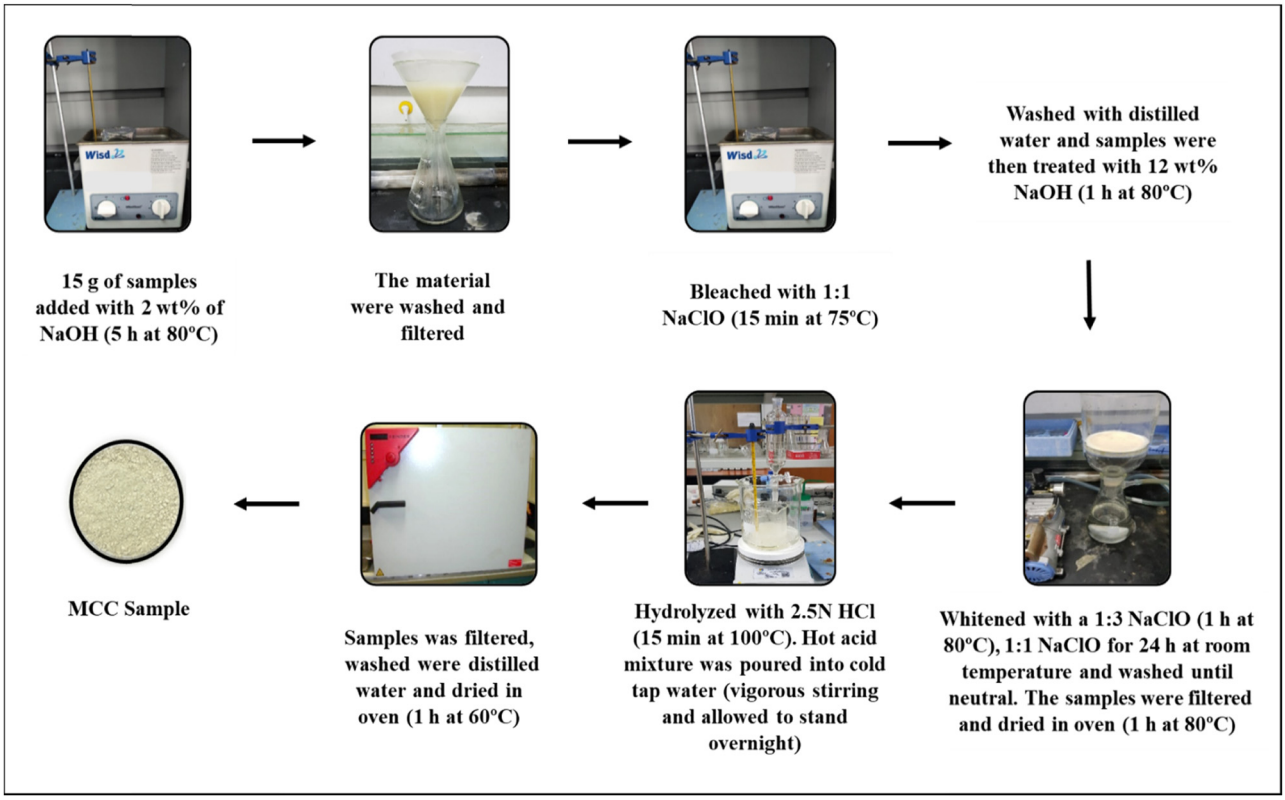

Figure 2: Procedures of preparation of MCC from pineapple leaves.

reached a constant mass. Step (3) The oven-dry sample was bleached at a ratio of 1:1 NaClO for 15 min at 75°C followed by washing with distilled water; the sample was then treated with 12 wt% of NaOH at 80°C for 1 h. Step (4) The samples obtained in step 3 were whitened with a 1:3 NaClO solution for 1 h at 75°C and then with a 1:1 NaClO solution for 24 h at room temperature before being washed until neutral. The samples were then filtered and dried for 1 h at 80°C. Step (5) The sample derived from step 4 was hydrolyzed with 2.5 N HCl for 15 min at 100°C. The hot acid mixture was poured into cold tap water with vigorous stirring and allowed to stand overnight. The sample was filtered, washed with distilled water, dried in the oven at 60°C for 1 h, and the sample obtained from step 5 was used for chemical and morphological studies. The preparation of NCC is shown as a graphical presentation in Figure 3.

2.3 Characterization of MCC and NCC from pineapple leaves

FTIR (Shimadzu IRPrestige-21) spectroscopy was used to determine the chemical properties and the molecular structural analysis. The KBr disc (ultra-thin pellets) approach was employed while taking the IR spectra. The samples were mixed with KBr (sample/KBr ratio, 1:100). The spectra were recorded in the range 500–4,000/cm with a resolution of 4/cm and a total of 32 scans for each sample was obtained. The crystalline phase of the MCC and NCC samples was evaluated using XRD (Bruker AXS-D8 Advance) at 40 kV and 40 mA with a wavelength of 0.15406 nm (λ). For each sample, the crystallinity index was determined using the following equation [37]:

$$\mathrm{CI}(\%) = \frac{I_{\mathrm{cry}} - I_{\mathrm{ams}}}{I_{\mathrm{cry}}} \times 100 \quad (1)$$

where CI is the crystallinity index (%), I_{cry} is the maximum intensity between 22° and 24°, and I_{ams} is the amorphous material intensity between the peaks at an angle of approximately 18° in the valley.

The crystallite size was inferred using the Scherrer equation (equation (2)) [38,39],

$$\text{crystallite size (nm)} = \frac{k\lambda}{\beta \cos\theta} \quad (2)$$

where k is the Scherrer constant (0.94), λ is the X-ray radiation wavelength, β is the full width at half-maximum (FWHM) of the diffraction peak, and θ is the corresponding Bragg angle.

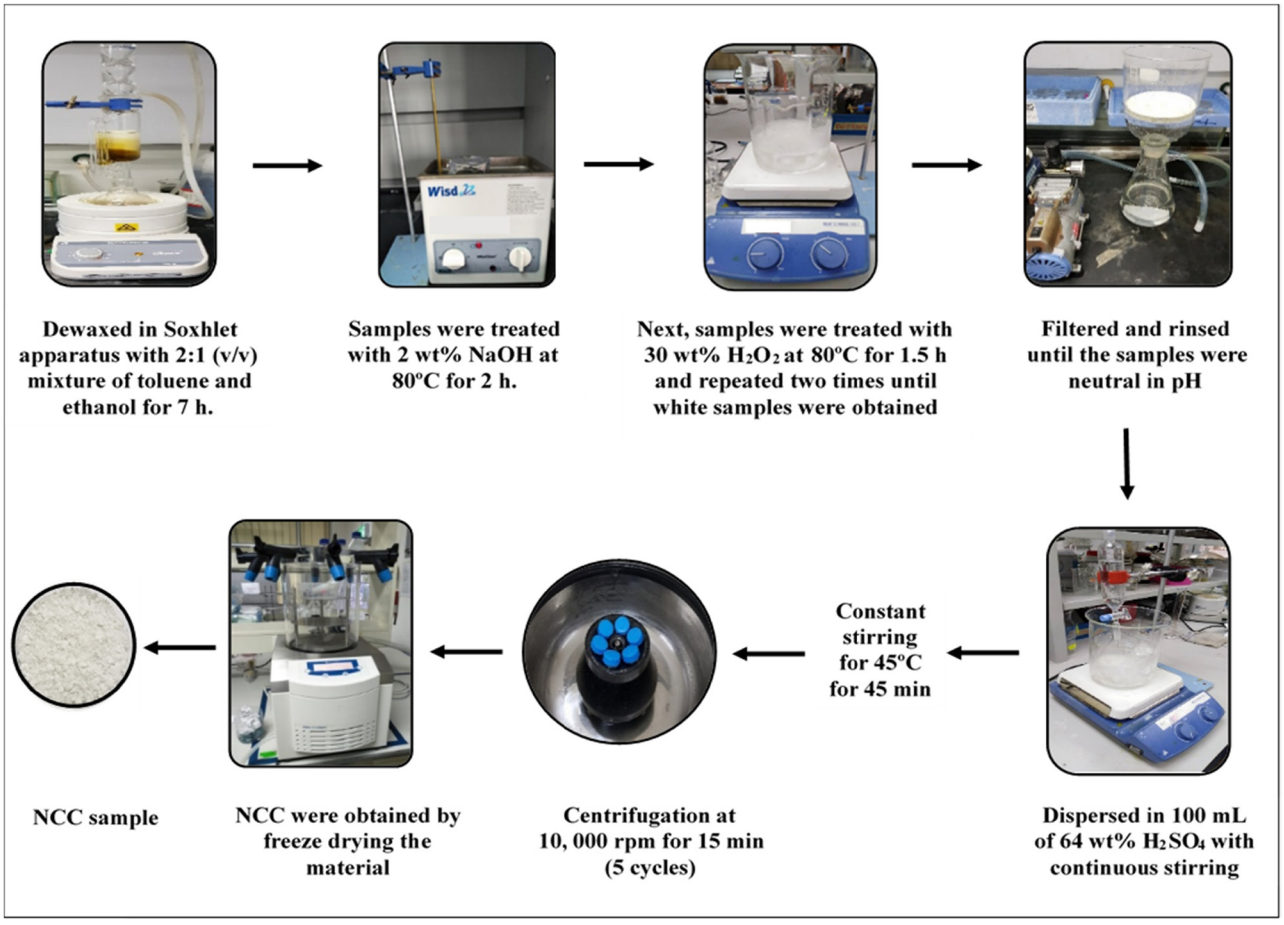

Figure 3: Procedures of preparation of NCC from pineapple leaves.

Morphological properties were studied using SEM and TEM. The surface of the NCC sample was coated with gold/palladium using a sputter coater device of Bal-Tec (MultiCoating System MED20), suggesting an excellent sample preparation technique. The sample was subjected to SEM (JEOL-JSM-6010LA) with an acceleration voltage of 15 kV. The diluted suspension of MCC and NCC was placed on a copper grid covered with a thin carbon film, stained with a 2 wt% of uranyl acetate solution, and dried at room temperature before subjecting to TEM. The dimension images of the MCC and NCC sample were observed using a TEM (JEM-2100F) operating at 80 kV of acceleration voltage.

2.4 Cytotoxicity studies

MRC-5 cells were cultured in RPMI 1640 containing foetal bovine serum (10%) and penicillin/streptomycin (10 mL) prior to cytotoxicity assay. MCC and NCC from ananas (pineapple) leaves and commercial MCC (1,000, 100, 10, 1, and 0.1 µg/mL) were dissolved in 4% NaOH solution prepared in deionized water, as treatment solutions. A 96 well plate for the treatment was filled with 90 µL of media containing MRC-5 cells and 10 µL of the treatment solution was added prior to the cytotoxicity assay. A 96 well plate for the treatment was filled with 90 µL of media containing MRC-5 cells and 10 µL of the treatment solution. The treatments were incubated in four replicates for 24, 48, and 72 h. MTT solution (50 µL) was added to each well and incubated at 37°C for 4 h [40]. DMSO (100 µL) then was added after the cells with MTT solution in each well were pipetted out. The absorbance reading at a wavelength of 570 nm was measured by using a plate reader. The cell viability was evaluated and was plotted by using GraphPad Prism 5.0. The findings from the cytotoxicity graph and GraphPad Prism 5.0 were collected and used to assess the treatment's absorbance reading. Using Student *t*-test analysis, the statistical significance between variables was tested in four replicates for each experiment, and p values ≤ 0.05 have been considered significant.

2.5 Molecular docking simulation

Molecular docking of cellobiose, the reducing unit of cellulose against human acid-beta-glucosidase (PDB: 1OGS), was carried out according to the instructions using the AutoDock 4.2 tool [41]. Briefly, the polar hydrogen atoms and the Kollman charges were assigned to the receptor protein. Partially Gasteiger charges were assigned to the ligand, and nonpolar hydrogen atoms were fused. A grid map of 40 × 40 × 40 Å with grid centre 23.05 70.77 −19.66 (*x*, *y*, and *z* positions, respectively) was used to cover the active site of protein structure to get the best conformational state of docking. The best docking pose was chosen based on the lowest binding energy (kcal/mol) values, and hydrogen and hydrophobic interactions were analyzed with Discovery Studio (v3.5). The LIGPLOT method was also used to build a 2-D graphical representation of the best-docked pose [42]. The amino acid residues involved in the formation of active pockets in the receptor for interaction with ligands/molecules, such as ARG2, THR21, ASN19, TYR22, ASN19, THR21, THR21, TYR22, THR21, THR21, TYR22, and VAL17, were identified based on a hetero atom co-crystallized with active sites of receptor already present in human acid beta-glucosidase (PDB: 1OGS).

3 Results and discussion

3.1 Structures of MCC and NCC from pineapple leaves

The isolated MCC and NCC powders from pineapple leaves are shown in Figure 4. Referring to the results, the MCC sample was found to be yellowish-white powder while the obtained NCC was a snowy white powder in colour. There is a difference in appearance for both samples when compared to the NCC sample. The colour of both samples changed from brown to light brown after alkaline treatment. The materials that were treated by the bleaching process appeared white for NCC and slightly yellowish-white for MCC. This visual is very important as it demonstrates that the non-cellulosic components and unwanted constituents throughout have been successfully eliminated by the chemical treatment process. The observed white colour also points out that the obtained samples are almost pure cellulosic materials. However, the texture of both samples is quite different. The difference in both MCC and NCC was influenced by the period of extraction and the suitability of the selected extraction method. Besides, referring to the literature, the processing conditions, nature of the selected plant sources, botanical origin, soil characteristics, and age of the plant also contribute differently to the amount of MCC and NCC residuals produced [43].

Both the obtained samples of MCC and NCC were successfully characterized by FTIR and XRD to evaluate their purity and crystallinity. In general, FTIR characterization depends on the atom vibrations in a molecule, and it can help to classify the functional groups within each of the samples available. The analysis of chemical structure is controlled by the chemical bonds that can vibrate, stretch, and bend. The main functional groups commonly present in cellulose samples, such as aromatic, esters, alcohols, alkanes, and ketones, can be identified by this spectroscopy analysis [44,45]. With high sensitivity, speed of data collection, and improved spectral precision, FTIR spectroscopy is one of the essential characterization studies in the study of MCC and NCC by referring to the wavelength and transmittance in IR radiation.

Figure 4: (a) Microcrystalline cellulose (MCC) and (b) nanocrystalline cellulose (NCC) derived from pineapple leaves.

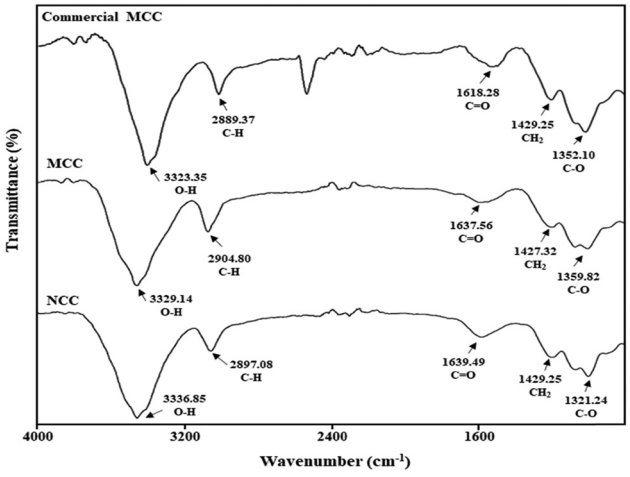

Figure 5: Fourier transform infrared spectra of commercial MCC, MCC, and NCC samples.

The alteration in the cellulose crystal structure leads to a reduction or loss in the intensity of certain FTIR peaks from the cellulose crystalline domains. The samples are expected to produce an absorbance region, and the infrared spectra for both MCC and NCC samples are studied based on the literature. The variation of absorptions peaks in the spectra exposed the different functional groups influenced by the modifications in the chemical composition of the fibres during the process of isolating MCC and NCC [46]. The FTIR results for commercial MCC, MCC, and NCC samples are displayed in Figure 5. Lignin and hemicelluloses were successfully eliminated by bleaching, alkali treatment, and acid hydrolysis, as determined by the FTIR spectra. Furthermore, no significant difference was found in both extracted MCC and NCC samples at the cellulose region.

Table 2 shows the functional groups of MCC and NCC, isolated from pineapple leaves, that were found in the FTIR spectra. Both samples of MCC and NCC showed almost similar spectra compare with the standard commercial MCC. The commercial MCC has functional groups of O–H at a wavelength of 3323.35/cm, C–H was observed at 2889.37/cm, C═O at 1618.28/cm, CH_2 at 1429.25/cm, and 1352.10/cm was assigned to C–O stretching. The strong dominant absorption peak associated with cellulose in extracted MCC and NCC occurs in the region from 3329.14 to 3336.85/cm, which points at the bending of the hydroxyl (O–H) groups and the stretching of hydrogen bonds to the cellulosic structure [47]. This appearance may be attributed to the absorption of moisture or water in the samples. Besides, the alkali treatment involved in the isolation of MCC and NCC reduces hydrogen bonding by removing the hydroxyl groups through a reaction with sodium hydroxide. This led to the increase in –OH concentration, evident from the increased intensity of the peak in the spectra. In both spectra, the characteristic band at about 2897.08–2904.80/cm is close to the C–H stretching vibration of alkyl groups in aliphatic bonds of cellulose, hemicellulose, and lignin [48].

The band between 1637.56 and 1639.49/cm was due to the carbonyl group (C═O) stretching vibration of the hemicellulose acetyl and uronic ester groups, or the lignin ferulic and p-coumaric acid carboxylic group [49]. Acid hydrolysis, which is required for the extraction of MCC and NCC from pineapple leaves, eliminates hemicellulose and lignin, resulting in a decrease in the strength of this peak in the cellulose spectrum. The bands that appeared at 1427.32 to 1429.25/cm are caused by CH_2 scissoring vibrating shift in MCC and NCC [50]. This peak was recognized as the crystallinity band in the samples and provides evidence of containing cellulose. Furthermore, both spectra of samples displayed the characteristic C–O stretching around 1321.24 to 1359.82/cm. The spectra of MCC and NCC, derived from pineapple leaves, revealed a comparable trend to the cellulose literature defining the O–H, C–H, C═O, CH_2, and C–O functional groups [51].

Another critical analysis that is useful for assessing the thermal stability of polymeric materials is thermogravimetric analysis. In evaluating the possible uses of MCC and NCC as biomedical products, thermal stability is an important parameter to be considered. The study of thermal degradation behaviour is significant for the performance of the materials and allowed researchers to optimize the composite design and treatment conditions to produce high-performance polymers with improved thermal stability. The thermal behaviour of the lignocellulosic materials depends on the treatment involved, source of raw materials, structure, chemical composition, and degree of crystallinity [52]. All samples revealed

Table 2: Functional groups of MCC and NCC from pineapple leaves

Samples of cellulose	–OH stretching (/cm)	C–H vibration (/cm)	C═O vibration (/cm)	CH_2 vibration (/cm)	C–O stretching (/cm)
Microcrystalline cellulose (MCC)	3329.14	2904.80	1637.56	1427.32	1359.82
Nanocrystalline cellulose (NCC)	3336.85	2897.08	1639.49	1429.25	1321.24

Table 3: XRD analysis for determining the crystallinity index (CI) and the crystallite size (nm) of MCC and NCC samples

Samples	Reflection at 2θ (°)	Crystallinity index (%)	Crystallite size (nm)
Microcrystalline cellulose (MCC)	14.5, 22, 34	75.00	4.52
Nanocrystalline cellulose (NCC)	15.5, 22, 35	76.38	4.70

water (moisture or chemically bonded) loss around 100°C and were attributed to dehydration during water removal [53].

Both MCC and NCC samples extracted from pineapple leaves displayed the same trend and pattern with the degradation occurring from 240 to 380°C in the second step. The exceptionally high slope for both samples is due to the depolymerization of the cellulose. The partial cross-linking of cellulose molecules reduces the degree of polymerization at this point, leading to the formation of CO, CO_2, H_2O, and a variety of hydrocarbon derivatives. The final steps revealed in this analysis show that rapid depolymerization occurs above a temperature of 350°C, and approximately about 70% of the weight loss. This finding is comparable with the results from Gan and co-workers that mentioned three main stages in the degradation profile [54].

The first initial weight loss component was found at about 50°C and approximately 100°C. The thermal stability of both MCC and NCC samples showed that the chemical treatment increased the temperature of degradation, influenced by the elimination of hemicelluloses and lignin. The higher degree of crystallinity also led to higher heat resistance and improved thermal degradation in MCC and NCC samples [55,56]. The residual mass at a temperature of 750°C for MCC samples is 6.13% while that of NCC samples is 14.98%. In comparison between the two samples, MCC showed a higher degradation temperature behaviour than the NCC from pineapple leaves, probably due to the variation in each MCC and NCC's outer surface structure derived from the different extraction techniques [57].

The crystallinity was measured by XRD. For the analysis of structural properties of MCC and NCC, the XRD technique was used to analyse the degree of crystallinity and the crystal structure of the cellulose samples. The preferred orientation of crystallites, also known as texture, is a significant factor to consider while analysing XRD. The texture development of the sample is frequently influenced by the synthesis techniques, the nature of the crystallites, and pretreatment. It is well known that the relative intensities of diffraction peaks are influenced by these factors and will affect the crystallinity index accordingly [58]. The X-ray diffraction pattern was obtained for both MCC and NCC samples isolated from pineapple leaves. Based on the results, it showed that the samples peaks at 2θ for MCC are 14.5°, 22° and 34° while those for NCC were around 15.5°, 22° and 35°. The samples' crystallinity index was calculated using the Segal method. Thompson and colleagues noted that Segal's method allows a rapid and simple way of determining crystallinity for cellulose and its derivatives [59]. Table 3 shows the XRD analysis of the MCC and NCC samples for the crystallinity index (CI) and the crystallite size (nm).

The crystalline structure of the samples is attributed to the primary X-ray diffractogram peaks, as illustrated in Figure 6, while the low intensity is attributed to the amorphous background of the cellulose samples. The XRD properties reveal a strong peak at 2θ = 22°, indicating higher crystallinity for both MCC and NCC samples. The sharp peaks of the graph suggest greater crystallinity activity for all the samples [60]. These peaks have a similar pattern and should resemble the typical cellulose I structure. Cellulose I is the most typical crystalline type, consisting of a series of crystallites and disordered amorphous regions. The significant intensity for both samples from this work was associated with the cellulose I crystalline structure of cellulose.

The crystallinity index of MCC, from pineapple leaves, was 75.00%, while NCC has 76.38% of crystallinity. As discussed in several studies, the crystallinity index provides a quantitative analysis of the crystallinity in powder, which can be related to the strength and stiffness of fibres [61]. Low crystallinity reveals a more disordered structure that results in a more amorphous powder,

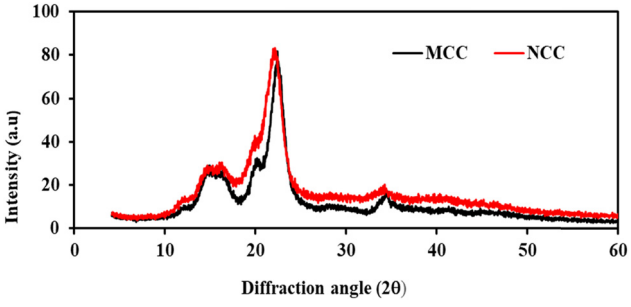

Figure 6: X-ray diffractograms of MCC and NCC from pineapple leaves.

whereas high crystallinity reveals an organized molecular structure that interprets small particles. The crystallite sizes of MCC and NCC that were determined by using the Scherrer equation were 4.52 and 4.70 nm, respectively. The crystallite size results support the description of the crystallinity behaviour of samples obtained.

Compounds of cellulose usually consist of lignin, hemicellulose, and α-cellulose. Cellulose is classified as crystalline in nature, while lignin is considered amorphous. The crystalline structure of cellulose is generally due to the interaction between the neighbouring molecule with the hydrogen bond and van der Waals forces [62]. This crystallinity characteristic is very important in terms of elasticity, rigidity, thermal stability, and also adsorption. According to the findings, it can be stated that the amorphous area of cellulose in MCC and NCC was targeted by the acid solution that was used in acid hydrolysis resulting in the increase of crystallinity index. The acid hydrolysis also eliminated polysaccharides, such as lignin matrix and hemicellulose that were bound in cellulose fibres, and the chains of MCC and NCC were rearranged. The results in the XRD crystallinity profile for MCC and NCC are significant to indicate the digestibility from the obtained samples [63].

3.2 Surface morphological analysis

Figure 7 shows the SEM micrograph of MCC and NCC samples isolated from pineapple leaves at x100 magnification. SEM is a good tool to investigate the morphological changes for both cellulose samples. From compositional analysis based on the literature, the raw pineapple leaves contain cellulose fibres bound by lignin and hemicellulose [64].

Based on the micrographs for both MCC and NCC, it appears to be composed of a compact structure. They displayed plenty of non-fibrous components spread across the fibre surface. The form of this sample shows an increase in its precise area, favours chemical response that includes acid hydrolysis. The agglomerated "rod-like" shape of the crystal structure increases the surface area and creates the reactivity of the fibres [65]. The compact agglomeration of MCC and NCC suggests intermolecular bonding of hydrogen and strong hydrophilic interaction between cellulose chains. During the bleaching treatment, most lignin is removed from the samples, and the reaction also facilitates in further defibrillation.

In this work, alkaline and bleaching treatments were involved in the isolation process of MCC and NCC for the pre-treatment of waste fibres. Bleaching leads to further defibrillation. Defibrillation occurs in the alkaline treatment and this trend increases in line with bleaching (whitening) treatment due to the expulsion of lignin and hemicellulose. Bleaching treatments can alter the surface of nanofibrils that look smoother than the untreated fibres [66]. Besides SEM analysis, TEM is also one of the good characterization techniques for analysing the morphological surface of nanometer-scale in MCC and NCC samples. The micrograph obtained by TEM allows visualization of the fibrils, which are organized in bundles by the strong attraction force of hydrogen bonds, showing further on the surface of their fibrils. The TEM micrographs as shown in Figure 8 illustrate the needle-like structure consisting mostly of single fibrils and some aggregates. A similar structure was obtained by Mahardika *et al.* [67] and Prado and Spinacé [68].

However, the size of both MCC and NCC is smaller than that reported in previous studies. This is because of the involvement of the acid hydrolysis process that removes the amorphous area of cellulosic microfibrils, maintaining intact straight crystalline domains [69]. The process of treatment inevitably decreases the size of the fibres to the nanometer scale. This finding is comparable to the work done by Teixeira and co-workers [70]. Nonetheless, the MCC and

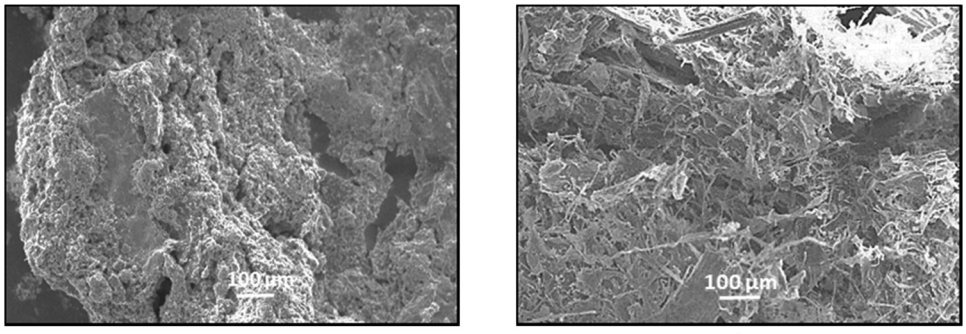

(a) (b)

Figure 7: SEM micrograph of (a) MCC and (b) NCC samples isolated from pineapple leaves.

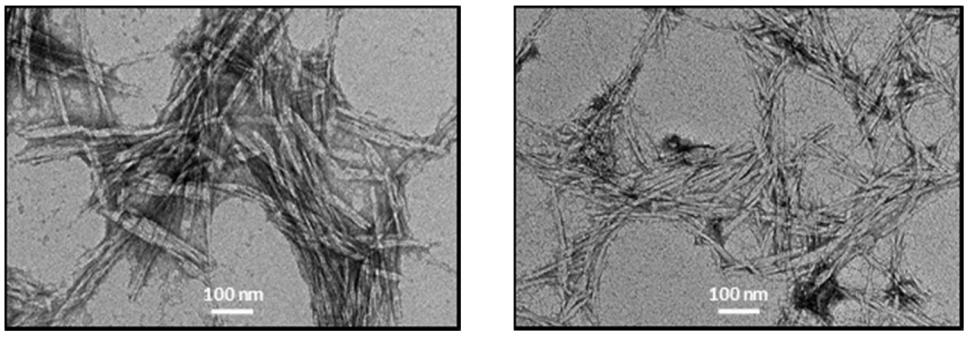

Figure 8: TEM micrographs of (a) MCC and (b) NCC samples isolated from pineapple leaves.

NCC agglomerates, as revealed from the TEM image, could be linked to the intermolecular hydrogen bonding between the cellulose.

Meanwhile, the hydrolysis with H_2SO_4 results in stable NCC aqueous suspension. The NCC surface hydroxyl groups are etherified with sulphate groups, alleviate the suspension by anionic repulsion forces, and have a low aggregation tendency [71]. Referring to the micrograph, it also depicts agglomeration of MCC and NCC bundles and points at dispersed crystallites and individual crystals. The needle-like shape of both samples is proof that the lignin and hemicellulose have been separated and eliminated by alkaline and bleaching (pre-treatment), and also acid hydrolysis causes the fibre bundles to be extracted into individual cellulose nanofibres.

3.3 Cytotoxicity effect of MCC and NCC on MRC-5 cells

Cytotoxicity test is an analysis for evaluating the cytotoxicity effect of compounds on the living organism *via* the cell viability assessment. This analysis is the simplest *in vitro* technique, which is a rapid and affordable approach for the initial biocompatibility safety evaluation of MCC and NCC materials. Since cellulose-based materials like MCC and NCC have considerable potential for medical applications, additional work is necessary to obtain further information on their toxicological and characteristics and their possible impacts on human health and safety. This cytotoxicity evaluation can be used as a vital aspect of nanomaterial characterization. MTT assays and MRC-5 cell lines were used to evaluating the cytotoxicity property of the biomaterials since this assay is largely used in the screening of toxic and harmless material compounds.

Figure 9(a–c), respectively, demonstrates the cytotoxicity activity of MCC and NCC against normal lung

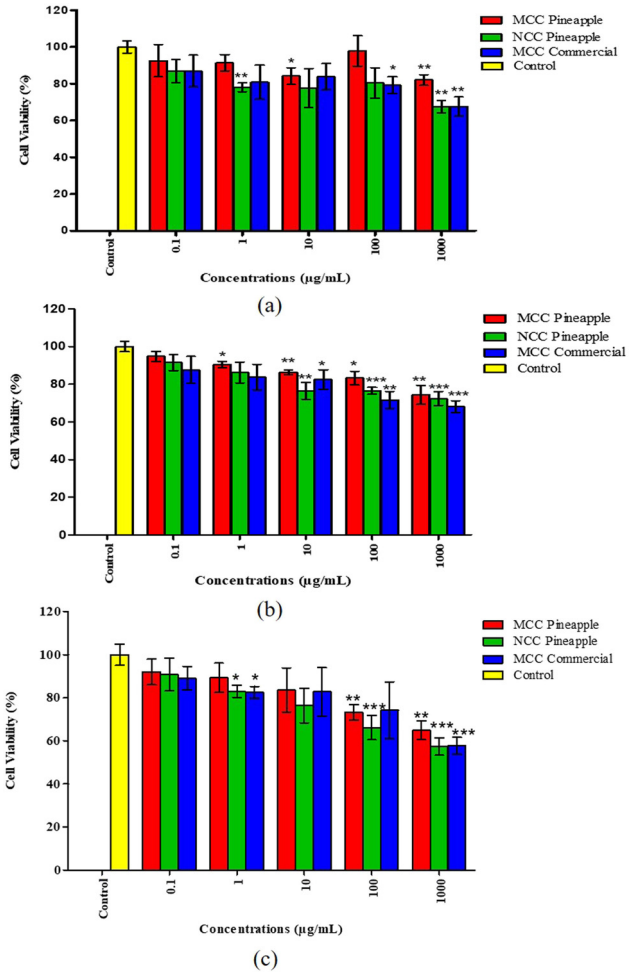

Figure 9: Cytotoxicity effect of MCC, NCC, and commercial MCC against human normal lung cells (MRC-5) for 24, 48, and 72 h of treatment. The analysis was performed using GraphPad Prism 5.0 and *t*-test analysis was done for each group. The * symbol indicates the significance level of the treatment, where *, **, and *** are $p < 0.05$, $p < 0.01$ and $p < 0.001$, respectively for treatments compared with the control of each group.

fibroblast cells (MRC-5). The percentage of cell viability in the medium was mainly dose-dependent. From Figure 9, it is shown that no significant difference in cell viability was observed at a concentration of 0.1 µg/mL relative to control for all cellulose types when exposed to different times. Different concentrations of MCC, NCC, and industrial MCC, ranging from 0.1, 1, 10, 100, and 1,000 µg/mL were tested on the viability of the cells and applied for 24, 48, and 72 h of treatment.

The results further showed that MCC and NCC had less toxicity to the MRC-5 cells after a 24 h treatment at lowest concentrations of 0.1, 1, and 10 µg/mL. On the other hand, MCC and NCC demonstrated cell inhibition below 30% at higher concentrations of 100 and 1,000 µg/mL. According to the findings, MCC, NCC, and commercial MCC significantly decreased cell viability at a concentration of 1,000 µg/mL between 70 and 52% compared to control except for MCC in 24 h treatment application. Furthermore, the research on cytotoxicity was investigated here to reveal that MCC and NCC from pineapple leaves were evaluated as less toxic compared to the commercialized MCC. The viability of MRC-5 cells in industrial MCC (1,000 µg/mL) and NCC (100 and 1,000 µg/mL) at 48 h of treatment was significantly lower ($p < 0.001$). The viability of MRC-5 cells for industrial MCC (100 µg/mL) and MCC (100 and 1,000 µg/mL) was significantly lower ($p < 0.001$) for 72 h of exposure. Besides, the viability of MRC-5 cells for commercial MCC (1,000 µg/mL) and NCC (100 and 1,000 µg/mL) was significantly different compared to the control. It also emerged from the results that the lowest concentrations (0.1, 1, and 10 µg/mL) of MCC and NCC were less toxic to MRC-5 cells with 24 h of treatment. At higher concentrations (100 and 1,000 µg/mL), the toxicity effect of MCC and NCC still showed cell inhibition below 30%. In spite of the cytotoxicity effects of MCC, NCC, and commercial MCC, the toxic effect was considered to be marginal as the inhibition of the treated MRC-5 cells did not exceed 50% inhibition concentration (IC_{50}).

According to previous studies, different treatments with MCC samples showed negligible toxicity to cell lines used with the lowest concentrations of treatments ranging from 10 to 250 µg/mL [72]. Thus, the results are consistent with the literature findings that indicate negligible cytotoxicity at lower concentrations of the treatments, against different cell lines [73]. In this analysis, we observed that the maximum concentration (1,000 µg/mL) for both cellulose samples showed less toxicity and had major cytotoxicity effects compared to control. Compared to MCC, NCC was typically slightly toxic due to its propensity to form a suspended gel when incubated at higher concentrations that could have blocked the

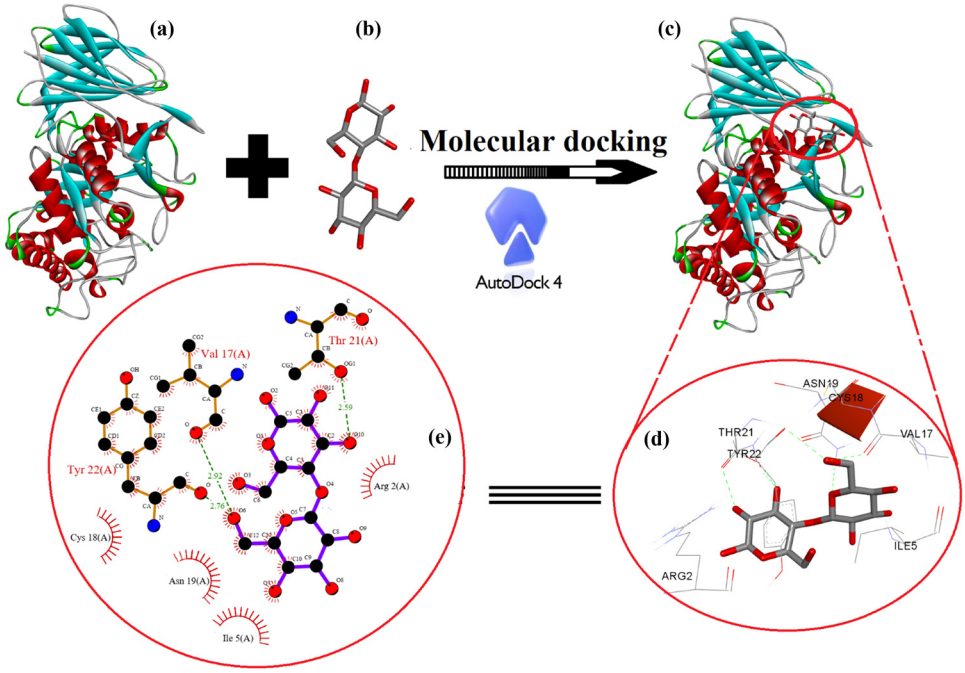

Figure 10: Molecular docking analysis between (a) human acid-beta-glucosidase (PDB: 1OGS) (b) cellulose unit (c), including the best-docked pose showing various interactions profiles and (d and e) 2D interaction diagram showing the active site participation in hydrogen such as hydrophobic and hydrophilic interactions.

passage of gases through the cell membranes. Meanwhile, at 48 and 72 h of incubation with the maximum concentrations of MCC and NCC (1,000 μg/mL), the percentage of cell viability decreased to 60%. This suggested that the MRC-5 cells may be nutrient deficient because of media condensation during incubation.

3.4 Molecular docking analysis

Figure 10 shows a graphical representation of the best docking pose with the receptor and the active binding pocket region. The lowest binding energy values (kcal/mol) and hydrogen/hydrophobic interaction analyses were used to examine cellulose- β-Glc docked complex (Figure 10c). The pose with the energy values (−5.0 kcal/mol) was found to be the best and most active conformational position. The pattern of hydrogen and hydrophobic contacts between the cellulosic unit and the target protein was investigated in more detail in the best-docked energy complex (10 D). The active amino acid pockets of enzymes such as ASN19, THR21, VAL17, and TYR22 are directly involved in hydrogen bonding with distances of 2.18, 1.63, 2.92, and 2.76 Å (Figure 10c and d).

Furthermore, hydrophobic and hydrophilic amino acids of the active site of the receptor, such as Cys18, Ile5, Asn19, and Arg2, were involved in stabilizing the docked pose of the cellulose unit and the enzyme complex in proper orientation *via* secondary forces such as van der Waals forces in order to use cellulose as a drug delivery carrier. Moreover, LIGPLOT was used to generate schematic 2D representations of ligand-receptor interactions for the best-docked pose, as shown in Figure 10e. The neighbouring amino acid residue in the pocket region, as shown in the 2D representation, is involved in hydrophobic and hydrophilic interactions to support the close contact of the ligand with the enzyme (red half circles) as well as the hydrogen bonding interaction between the receptor and the ligand (green bonds).

4 Conclusion

In this study, the cytotoxicity effects of MCC and NCC from pineapple leaves to normal fibroblast cells in the lungs (MRC-5) were assessed. The cytotoxicity effect of MCC and NCC revealed low toxicity for 24, 48, and 72 h of treatment at higher concentrations. The obtained MCC and NCC were of high purity and high crystallinity based on the characterization studies. The morphology of needle-like shapes proved that these materials have a nanoscale of aspect ratio in length and diameter. The crystallinity index of cellulose from the pineapple leaves gives NCC a higher crystallinity compared with the MCC samples. The difference in findings of physical properties and sample crystallinity may be due to the different pretreatment techniques and hydrolysis of acids. Overall, the obtained MCC and NCC from pineapple leaves are an effective option for sustainable natural resource production in Malaysia, which are safe and biologically compatible to be used as a drug delivery carrier in pharmaceutical applications. A molecular docking analysis will provide a deeper understanding of the relationship between cellulose and receptor proteins/enzymes, which is useful for researching drug delivery pathways in biological systems.

Funding information: The authors acknowledge the support from the Centre of Research and Instrument Management (CRIM), Universiti Kebangsaan Malaysia and Ministry of Higher Education Malaysia, under grants MI-2019-018 and DIP-2015-028 and Taif University Researchers Supporting Project number (TURSP-2020/45) Taif University, Taif, Saudi Arabia.

Author contributions: All authors have accepted responsibility for the entire content of this manuscript and approved its submission.

Conflict of interest: The authors state no conflict of interest.

References

[1] Patra JK, Das G, Fraceto LF, Campos EVR, Rodriguez-Torres MDP, Acosta-Torres LS, et al. Nano based drug delivery systems: recent developments and future prospects. J Nanobiotechnology. 2018;16(1):1–33.
[2] Amin MCIM, Abadi AG, Ahmad N, Katas H, Jamal JA. Bacterial cellulose film coating as drug delivery system: physicochemical, thermal and drug release properties. Sains Malaysiana. 2012;41(5):561–68.
[3] Jian W, Hui D, Lau D. Nanoengineering in biomedicine: current development and future perspective. Nanotechnol Rev. 2020;9(1):700–15.
[4] Dias F, Duarte C. Cellulose and its derivatives use in the pharmaceutical compounding practice. Cellul – Med Pharm Electron Appl. 1st ed. 2013. p. 141–62.
[5] Lin N, Dufresne A. Nanocellulose in biomedicine: current status and future prospect. Eur Polym J. 2014;59:302–25.
[6] Halib N, Ahmad I. Nanocellulose: insight into health and medical applications. Handb Ecomater. 2019;2:1345–56.

[7] Yu T, Soomro SA, Huang F, Wei W, Wang B, Zhou Z, et al. Naturally or artificially constructed nanocellulose architectures for epoxy composites: a review. Nanotechnol Rev. 2020;9(1):1643–59.
[8] Plackett D, Letchford K, Jackson J, Burt H. A review of nanocellulose as a novel vehicle for drug delivery. Nord Pulp Pap Res J. 2014;29(1):105–18.
[9] Kargarzadeh H, Ahmad I, Abdullah I, Dufresne A, Zainudin SY, Sheltami RM. Effects of hydrolysis conditions on the morphology, crystallinity, and thermal stability of cellulose nanocrystals extracted from kenaf bast fibers. Cellulose. 2012;19(3):855–66.
[10] Santos RM, dos Flauzino Neto WP, Silvério HA, Martins DF, Dantas NO, Pasquini D. Cellulose nanocrystals from pineapple leaf, a new approach for the reuse of this agro-waste. Ind Crop Prod. 2013;50:707–14.
[11] Sheltami RM, Abdullah I, Ahmad I, Dufresne A, Kargarzadeh H. Extraction of cellulose nanocrystals from mengkuang leaves (Pandanus tectorius). Carbohydr Polym. 2012;88(2):772–79.
[12] Yang J, Han CR. Mechanically viscoelastic properties of cellulose nanocrystals skeleton reinforced hierarchical composite hydrogels. Appl Mater Interfaces. 2016;8(38):25621–30. doi: 10.1021/acsami.6b08834.
[13] Qian S, Tao Y, Ruan YP, Fontanillo Lopez CA, Xu LQ. Ultrafine bamboo-char as a new reinforcement in poly(lactic acid)/bamboo particle biocomposites: the effects on mechanical, thermal, and morphological properties. J Mater Res. 2018;33(22):3870–79.
[14] Prasenjit D, Prasanta D, Abhijit C, Tejendra B. A survey on pineapple and its medicinal value. Sch Acad J Pharm. 2012;1(1):24–9.
[15] Ibrahim NA, Azraaie N, Zainul Abidin NAM, Mamat Razali NA, Abdul Aziz F, Zakaria S. Preparation and characterization of alpha cellulose of pineapple (*Ananas comosus*) leaf fibres (PALF). Adv Mater Res. 2014;895:147–50.
[16] Trilokesh C, Uppuluri KB. Isolation and characterization of cellulose nanocrystals from jackfruit peel. Sci Rep. 2019;9(1):1–8.
[17] Sainorudin MH, Mohammad M, Kadir NHA, Abdullah NA, Yaakob Z. Characterization of several microcrystalline cellulose (MCC)-based agricultural wastes via x-ray diffraction method. Solid state phenomena. Vol. 280. Trans Tech Publications Ltd; 2018.
[18] Tripathy DB, Mishra A. Renewable plant-based raw materials for industry. In: Scott RA, editor. Encyclopedia of inorganic and bioinorganic chemistry. Hoboken, New Jersey: John Wiley & Sons, Ltd; 2016. p. 1–16.
[19] Asim M, Abdan K, Jawaid M, Nasir M, Dashtizadeh Z, Ishak MR, et al. A review on pineapple leaves fibre and its composites. Int J Polym Sci. 2015;2015:1–16.
[20] Boschetti WTN, Carvalho AMML, Carneiro AdCO, Vidaurre GB, Gomes FJB, Soratto DN. Effect of mechanical treatment of eucalyptus pulp on the production of nanocrystalline and microcrystalline cellulose. Sustainability. 2021;13:5888.
[21] Liu Y, Liu A, Ibrahim SA, Yang H, Huang W. Isolation and characterization of microcrystalline cellulose from pomelo peel. Int J Biol Macromol. 2018;111:717–21.
[22] Kian LK, Jawaid M, Ariffin H, Alothman OY. Isolation and characterization of microcrystalline cellulose from roselle fibers. Int J Biol Macromol. 2017;103:931–40.
[23] Agblevor FA, Ibrahim MM, El-Zawawy WK. Coupled acid and enzyme mediated production of microcrystalline cellulose from corn cob and cotton gin waste. Cellulose. 2007;14:247–56.
[24] Trache D, Donnot A, Khimeche K, Benelmir R, Brosse N. Physico-chemical properties and thermal stability of microcrystalline cellulose isolated from Alfa fibres. Carbohydr Polym. 2014;104:2230–6.
[25] Haafiz MM, Hassan A, Zakaria Z, Inuwa IM. Isolation and characterization of cellulose nanowhiskers from oil palm biomass microcrystalline cellulose. Carbohydr Polym. 2014;103:119–25.
[26] de Oliveira RL, da Silva Barud H, de Assunçao RM, da Silva Meireles C, Carvalho GO, Filho GR, et al. Synthesis and characterization of microcrystalline cellulose produced from bacterial cellulose. J Therm Anal Calorim. 2011;106:703–09.
[27] Aprilia SNA, Arahman N. Properties of nanocrystalline cellulose from pineapple crown leaf waste. IOP Conf Ser: Mater Sci Eng. 2020;796:012007.
[28] Camacho M, Corrales Ureña YR, Lopretti M, Carballo LB, Moreno G, Alfaro B, et al. Synthesis and characterization of nanocrystalline cellulose derived from pineapple peel residues. J Renew Mater. 2017;5:271–9.
[29] Karakehya N, Bilgiç C. Preparation of nanocrystalline cellulose from tomato stem and commercial microcrystalline cellulose: a comparison between two starting materials. Cell Chem Technol. 2019;53:993–1000.
[30] Giri J, Lach R, Sapkota J, Susan MABH, Saiter JM, Henning S, et al. Structural and thermal characterization of different types of cellulosic fibers. BIBECHANA. 2019;16:177–86.
[31] Islam MS, Kao N, Bhattacharya SN, Gupta R, Choi HJ. Potential aspect of rice husk biomass in Australia for nanocrystalline cellulose production. Chin J Chem Eng. 2018;2018(26):465–76.
[32] Sukyai P, Anongjanya P, Bunyahwuthakul N, Kongsin K, Harnkarnsujarit N, Sukatta U, et al. Effect of cellulose nanocrystals from sugarcane bagasse on whey protein isolate-based films. Food Res Int. 2018;107:528–35.
[33] Ilyas RA, Sapuan SM, Ishak MR. Isolation and characterization of nanocrystalline cellulose from sugar palm fibres (Arenga Pinnata). Carbohydr Polym. 2018;181:1038–51.
[34] Ventura-Cruz S, Flores-Alamo N, Tecante A. Preparation of microcrystalline cellulose from residual Rose stems (*Rosa* spp.) by successive delignifcation with alkaline hydrogen peroxide. Int J Biol Macromol. 2020;155:324–9.
[35] Abu-Thabit NY, Judeh AA, Hakeem AS, Ul-Hamid A, Umar Y, Ahmad A. Isolation and characterization of microcrystalline cellulose from date seeds (*Phoenix dactylifera* L.). Int J Biol Macromolecules. 2020;155:730–9.
[36] Singanusong R, Tochampa W, Kongbangkerd T, Sodchit C. Extraction and properties of cellulose from banana peels. Suranaree J Sci Technol. 2013;21:14.
[37] Segal L, Creely JJ, Martin AE, Conrad CM. An empirical method for estimating the degree of crystallinity of native cellulose using the x-ray diffractometer. Text Res J. 1959;29(10):786–94.
[38] He J, Tang Y, Wang SY. Differences in morphological characteristics of bamboo fibres and other natural cellulose fibres: Studies on X-ray diffraction, solid state ^{13}C-CP/MAS NMR, and second derivative FTIR spectroscopy data. Iran Polym J (Engl Ed). 2007;16(12):807–18.

[39] El-Denglawey A. Illumination effect on the structural and optical properties of nano meso nickel (II) tetraphenyl-21H, 23H-porphyrin films induces new 2 h photo bleached optical sensor. J Lumin. 2018;194:381–6.
[40] Al-Nasiry S, Hanssens M, Luyten C, Pijnenborg R. The use of Alamar Blue assay for quantitative analysis of viability, migration and invasion of choriocarcinoma cells. Hum Reprod. 2007;22(5):1304–9.
[41] Morris GM, Huey R, Lindstrom W, Sanner MF, Belew RK, Goodsell DS, et al. AutoDock4 and autodocktools4: automated docking with selective receptor flexibility. J Comput Chem. 2009;30:2785–91.
[42] Wallace AC, Laskowski RA, Thornton JM. LIGPLOT: a program to generate schematic diagrams of protein-ligand interactions. Protein Eng. 1995;8:127–34.
[43] Shanmugam N, Nagarkar RD, Kurhade M. Microcrystalline cellulose powder from banana pseudostem fibres using biochemical route. Indian J Nat Prod Resour. 2015;6(1):42–50.
[44] Mat Zain NF. Preparation and characterization of cellulose and nanocellulose from pomelo (citrus grandis) albedo. J Nutr Food Sci. 2014;5(1):10–3.
[45] Wulandari WT, Rochliadi A, Arcana IM. Nanocellulose prepared by acid hydrolysis of isolated cellulose from sugarcane bagasse. IOP Conf Ser Mater Sci Eng. 2016;107(1):012045.
[46] Adel AM, El-Shafei AM, Ibrahim AA, Al-Shemy MT. Chitosan/nanocrystalline cellulose biocomposites based on date palm (*Phoenix dactylifera* L.) sheath fibers. J Renew Mater. 2019;7(6):567–82.
[47] Hishikawa Y, Togawa E, Kondo T. Characterization of individual hydrogen bonds in crystalline regenerated cellulose using resolved polarized FTIR spectra. ACS Omega. 2017;2:1469–76.
[48] Li M, Wang LJ, Li D, Cheng YL, Adhikari B. Preparation and characterization of cellulose nanofibers from de-pectinated sugar beet pulp. Carbohydr Polym. 2014;102(1):136–43.
[49] Rashid M, Gafur MA, Sharafat MK, Minami H, Miah MAJ, Ahmad H. Biocompatible microcrystalline cellulose particles from cotton wool and magnetization via a simple in situ co-precipitation method. Carbohydr Polym. 2017;170:72–9.
[50] Lee KY, Aitomäki Y, Berglund LA, Oksman K, Bismarck A. On the use of nanocellulose as reinforcement in polymer matrix composites. Compos Sci Technol. 2014;105:15–27.
[51] Huntley CJ, Crews KD, Curry ML. Chemical functionalization and characterization of cellulose extracted from wheat straw using acid hydrolysis methodologies. Int J Polym Sci. 2015;2015:1–9.
[52] Fisher T, Hajaligol M, Waymack B, Kellogg D. 27-pyrolysis behavior and kinetics of biomass derived materials. J Anal Appl Pyrolysis. 2002;62:331–49.
[53] Moreno G, Ramirez K, Esquivel M, Jimenez G. Isolation and characterization of nanocellulose obtained from industrial crop waste resources by using mild acid hydrolysis. J Renew Mater. 2018;6:362–69.
[54] Gan PG, Sam ST, Faiq M, Omar MF. Thermal properties of nanocellulose-reinforced composites: a review. J Appl Polym Sci. 2020;137:48544.
[55] Santmartí A, Lee KY. Crystallinity and thermal stability of nanocellulose. Nanocellulose and sustainability. CRC Press; 2018. p. 67–86
[56] Sainorudin MH, Abdullah NA, Rani MSA, Mohammad M, Abd Kadir NH, Razali H, et al. Investigation of the structural, thermal and morphological properties of nanocellulose synthesised from pineapple leaves and sugarcane bagasse. Curr Nanosci. 2021;17:1875–86.
[57] Indarti E, Marwan, Wanrosli WD. Thermal stability of oil palm empty fruit bunch (OPEFB) nanocrystalline cellulose: effects of post-treatment of oven drying and solvent exchange techniques. J Phys Conf Ser. 2015;622:622.
[58] Flórez Pardo LM, Salcedo Mendoza JG, López Galán JE. Influence of pretreatments on crystallinity and enzymatic hydrolysis in sugar cane residues. Braz J Chem Eng. 2019;36(1):131–41.
[59] Thompson L, Azadmanjiri J, Nikzad M, Sbarski I, Wang J, Yu A. Cellulose nanocrystals: production, functionalization and advanced applications. Rev Adv Mater Sci. 2019;58:1–16.
[60] Zhang D, Zhang Q, Gao X, Piao G. A nanocellulose polypyrrole composite based on tunicate cellulose. Int J Polym Sci. 2013;2013:1–6.
[61] Azubuike CP, Okhamafe AO. Physicochemical, spectroscopic and thermal properties of microcrystalline cellulose derived from corn cobs. Int J Recycl Org Waste Agric. 2012;1(1):9.
[62] Nishiyama Y. Molecular interactions in nanocellulose assembly subject areas. Phil Trans R Soc A. 2017;376:20170047.
[63] Park S, Baker JO, Himmel ME, Parilla PA, Johnson DK. Cellulose crystallinity index: measurement techniques and their impact on interpreting cellulase performance. Biotechnol Biofuels. 2010;3:1–10.
[64] Sun JX, Sun XF, Zhao H, Sun RC. Isolation and characterization of cellulose from sugarcane bagasse. Polym Degrad Stab. 2004;84(2):331–9.
[65] Saba N, Jawaid M. Recent advances in nanocellulose-based polymer nanocomposites. In: Cellulose-reinforced nanofiber composites: production, properties and applications. Woodhead publishing series in composites science and engineering. Woodhead Publishing, Elsevier Ltd; 2017. p. 89–112.
[66] Marwah R, Ibrahim NA, Zainuddin N, Saad WZ, Razak NIA, Chieng BW. The effect of fiber bleaching treatment on the properties of poly(lactic acid)/oil palm empty fruit bunch fiber composites. Int J Mol Sci. 2014;15(8):14728–42.
[67] Mahardika M, Abral H, Kasim A, Arief S, Asrofi M. Production of nanocellulose from pineapple leaf fibers via high-shear homogenization and ultrasonication. Fibers. 2018;6(2):1–12.
[68] Prado KS, Spinacé MAS. Isolation and characterization of cellulose nanocrystals from pineapple crown waste and their potential uses. Int J Biol Macromol. 2019;122:410–6.
[69] Yang J, Ching YC, Chuah CH. Applications of lignocellulosic fibers and lignin in bioplastics: a review. Polym (Basel). 2019;11(5):1–26.
[70] Teixeira JG, Gomes MG, Oliveira RR, Silva VA, Mariana M, Ortiz AB, et al. Sugarcane bagasse ash reinforced hdpe composites: effects of electron-beam radiation crosslinking on tensile and morphological properties. In International Nuclear Atlantic Conference – INAC. 2013.
[71] Zeni M, Favero D, Pacheco K, Ana Grisa M. Preparation of microcellulose (MCC) and nanocellulose (NCC) from Eucalyptus Kraft Ssp Pulp. Polym Sci. 2015;1:1–7.
[72] Hanif Z, Ahmed FR, Shin SW, Kim YK, Um SH. Size- and dose-dependent toxicity of cellulose nanocrystals (CNC) on human fibroblasts and colon adenocarcinoma. Colloids Surf B Biointerfaces. 2014;119:162–5.
[73] Menas AL, Yanamala N, Farcas MT, Russo M, Friend S, Fournier PM, et al. Fibrillar vs crystalline nanocellulose pulmonary epithelial cell responses: cytotoxicity or inflammation? Chemosphere. 2017;171:671–80.